

## Supporting Information

### **An overall water-splitting polyoxometalate catalyst for the electromicrobial conversion of CO<sub>2</sub> in neutral water**

*Meng Wang, Wei Zhong, Shuangshuang Zhang, Rongji Liu, Jianmin Xing, and Guangjin Zhang\**

**Figure S1.** Energy-dispersive X-ray spectrum (EDS) combined with SEM images.

**Figure S2.** (a) Cu 2p, (b) Co 2p, (c) P 2p and (d) W 4f XPS spectra of as-prepared Cu<sub>6</sub>Co<sub>7</sub>/CC powder and Cu<sub>6</sub>Co<sub>7</sub>/CC film.

**Figure S3.** I-t curves for HER and H<sub>2</sub> evolving.

**Figure S4.** I-t curves for OER.

**Figure S5.** Linear sweep voltammetry curves of the ORR for Cu<sub>6</sub>Co<sub>7</sub>/CC after HER test (black) and Pt/C/CC (red) in O<sub>2</sub> saturated in phosphate buffer (pH 7) at a scan rate of 10 mV/s.

**Figure S6.** SEM images of Cu<sub>6</sub>Co<sub>7</sub>/CC after HER test (a) and OER test (b).

**Figure S7.** (a) Cu 2p, (b) Co 2p, (c) P 2p and (d) W 4f XPS spectra of  $\text{Cu}_6\text{Co}_7/\text{CC}$  after HER and OER tests.

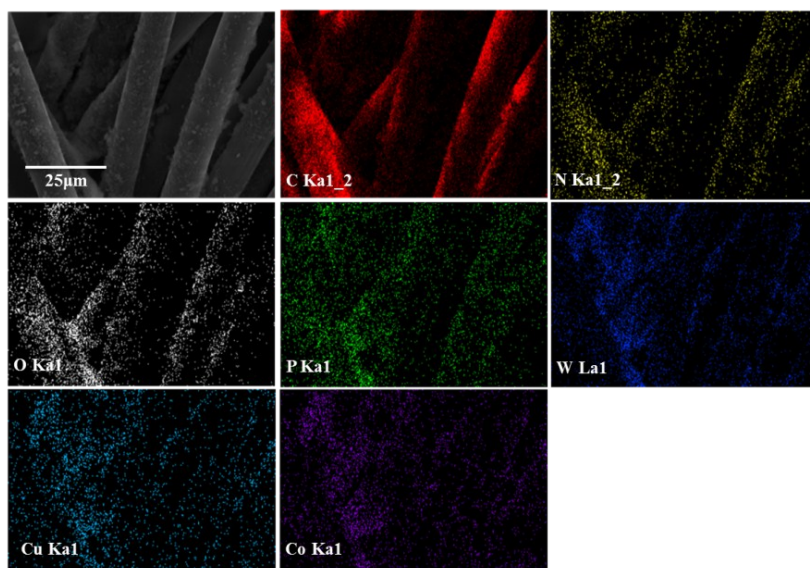
**Figure S8.** XRD spectra of  $\text{Cu}_6\text{Co}_7/\text{CC}$  after HER and OER tests.

**Figure S9.** SEM images of  $\text{Cu}_6\text{Co}_7/\text{CC}$  after the overall water splitting reaction ( (a) anode, (b) cathode) .

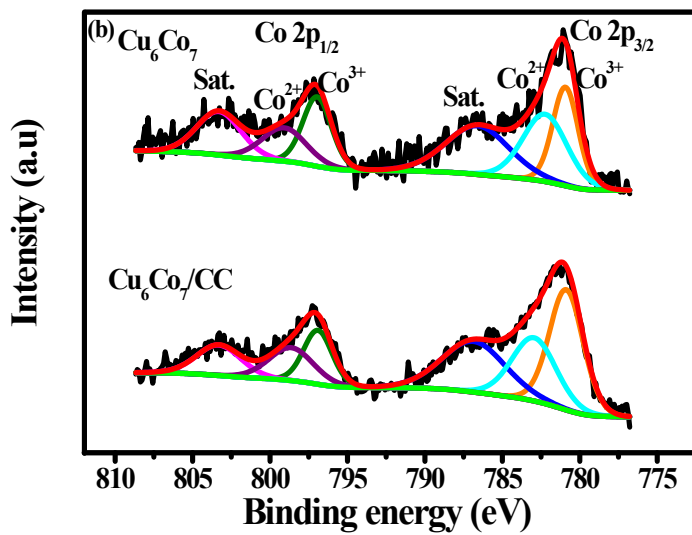
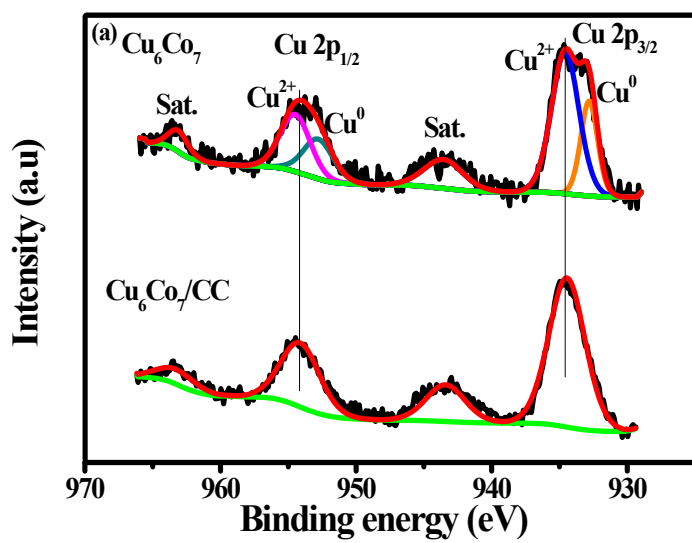
**Figure S10.** The dependence of the growth of *R. eutropha* on hydrogen evolution during the electrolysis with  $\text{CO}_2$  ( $E_{\text{appl}}=1.8 \text{ V}$ ) .

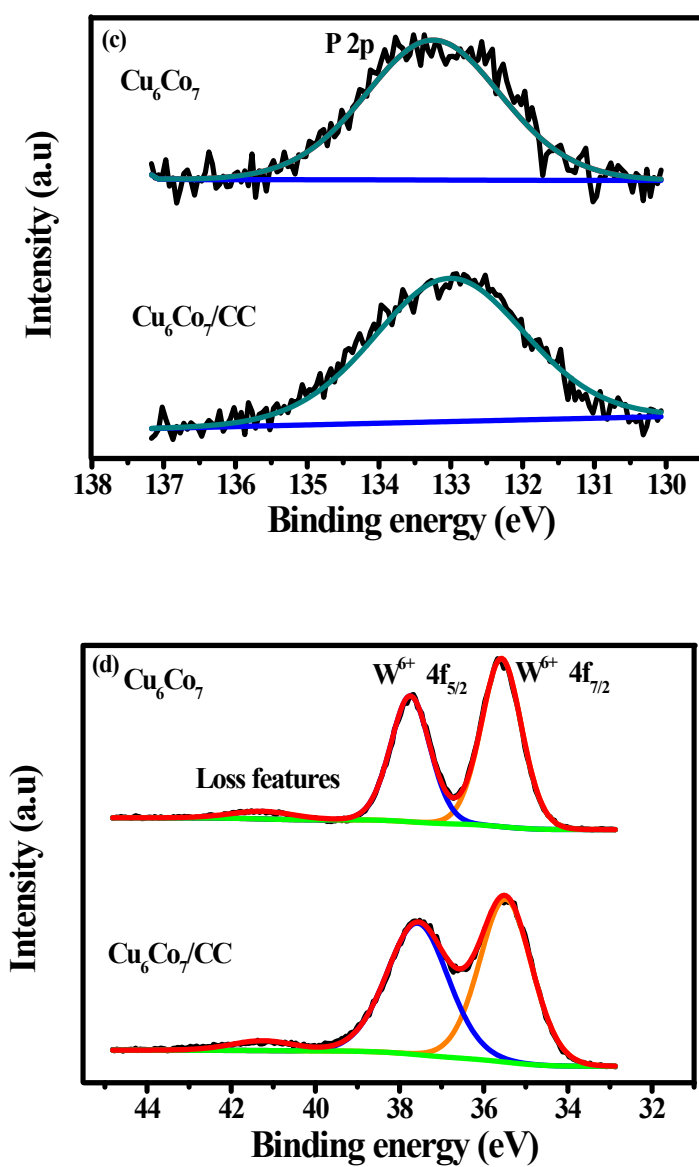
**Table S1.** Comparison of HER performances of different catalysts under neutral conditions.

**Table S2.** Comparison of the performance of  $\text{Cu}_6\text{Co}_7/\text{CC}$  to other bioelectrochemical systems for  $\text{CO}_2$  fixation.

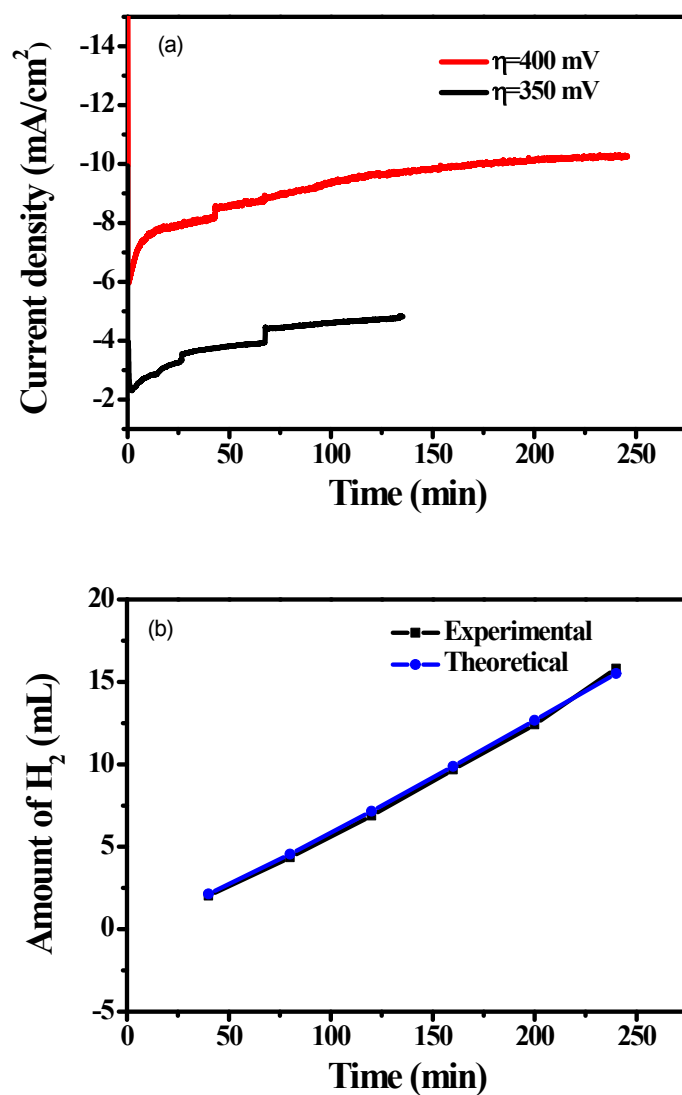


**Figure S1.** Energy-dispersive X-ray spectrum (EDS) combined with SEM images of the Cu<sub>6</sub>Co<sub>7</sub>/CC film.

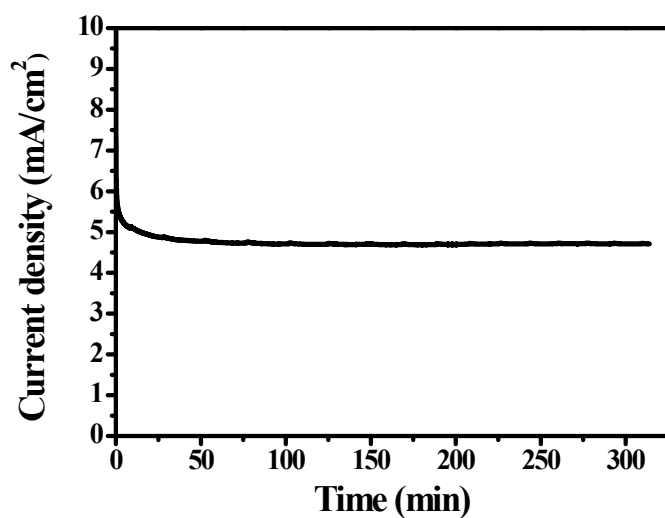




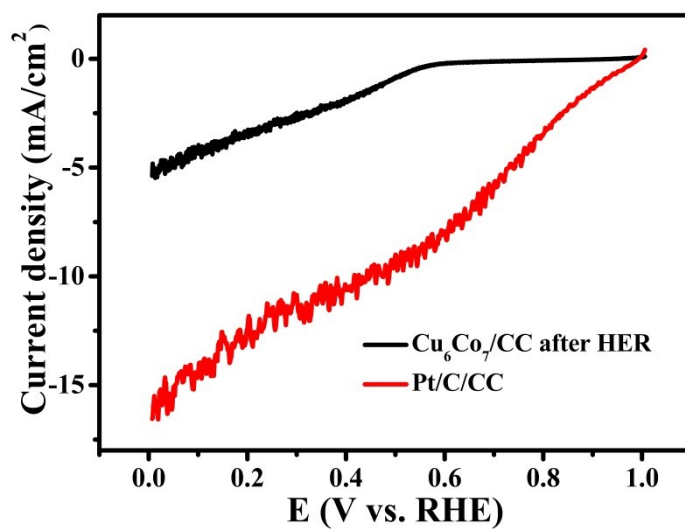
**Figure S2.** (a) Cu 2p, (b) Co 2p, (c) P 2p and (d) W 4f XPS spectra of as-prepared  $\text{Cu}_6\text{Co}_7/\text{CC}$  powder and  $\text{Cu}_6\text{Co}_7/\text{CC}$  film.



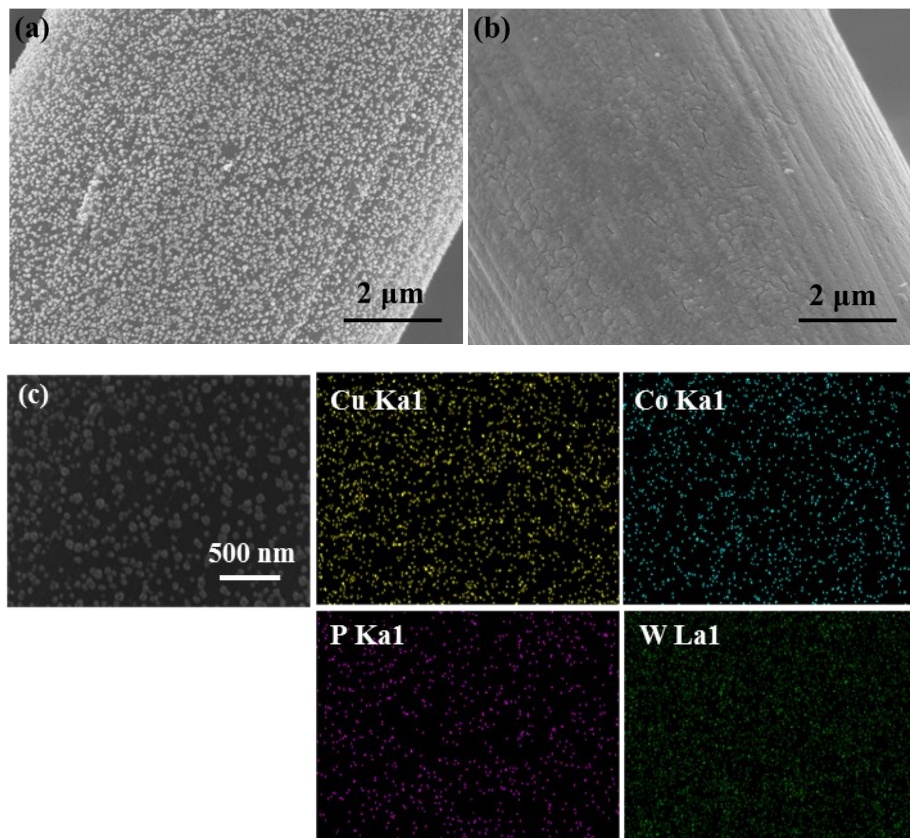
**Figure S3.** (a) I-t curves for Cu<sub>6</sub>Co<sub>7</sub>/CC at a fixed overpotential of 400 and 350 mV for HER proves, (b) The theoretically calculated and experimentally measured amount of evolved hydrogen during electrolysis process at an overpotential of 400 mV.



**Figure S4.** I-t curves for Cu<sub>6</sub>Co<sub>7</sub>/CC at a fixed overpotential of 400 mV for OER.

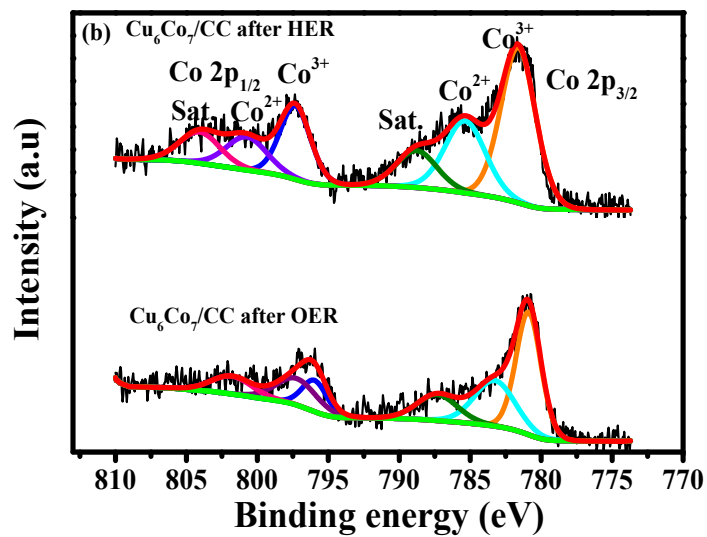
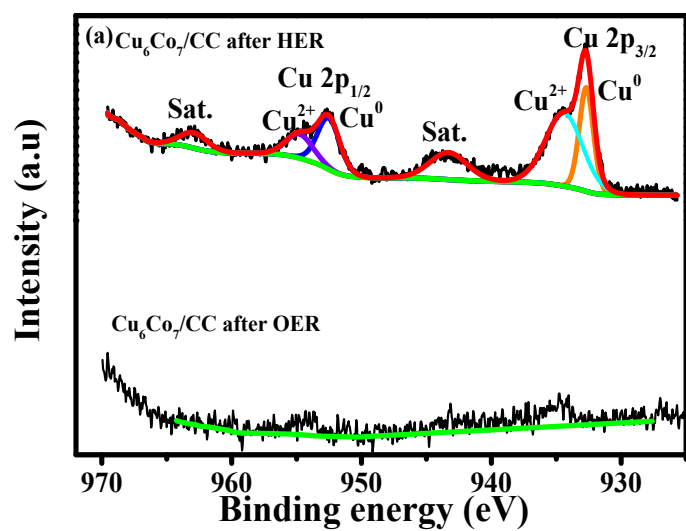


**Figures S5.** Linear sweep voltammetry curves of the ORR for Cu<sub>6</sub>Co<sub>7</sub>/CC after HER test (black) and Pt/C/CC (red) in O<sub>2</sub> saturated in phosphate buffer (pH 7) at a scan rate of 10 mV/s.



**Figure S6.** SEM images of Cu<sub>6</sub>Co<sub>7</sub>/CC after HER (a) and OER tests (b), (c) EDS combined with SEM images of the Cu<sub>6</sub>Co<sub>7</sub>/CC after HER test.





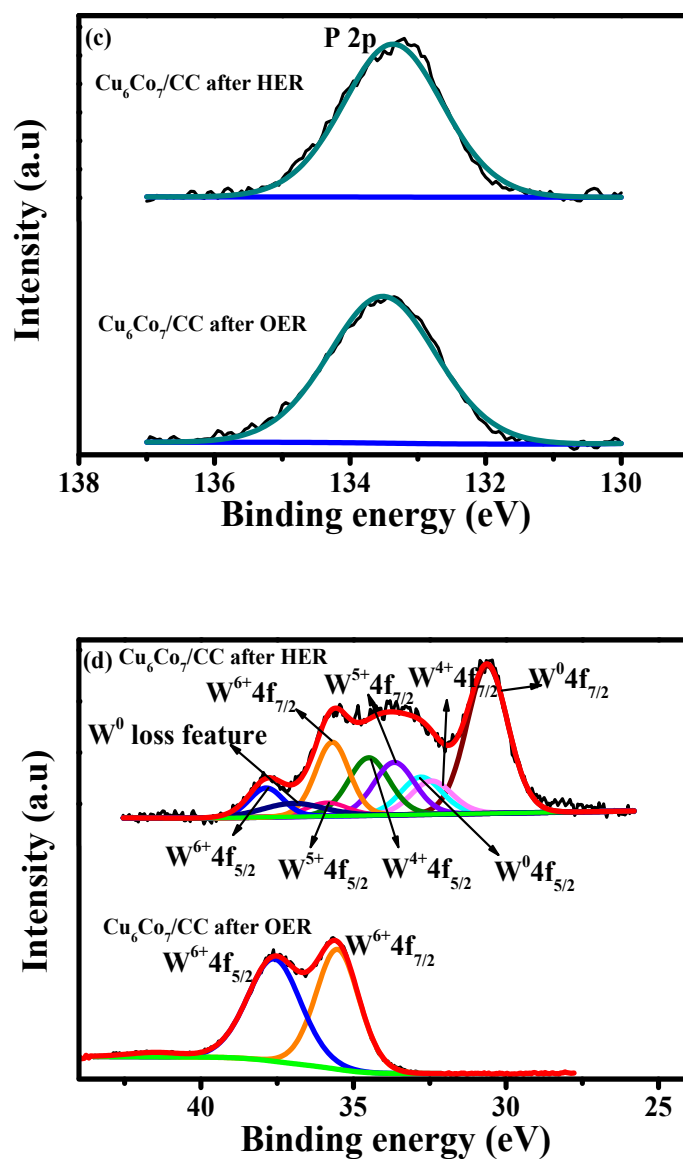


**Figure S7.** (a) Cu 2p, (b) Co 2p, (c) P 2p and (d) W 4f XPS spectra of  $\text{Cu}_6\text{Co}_7/\text{CC}$  after HER and OER tests.

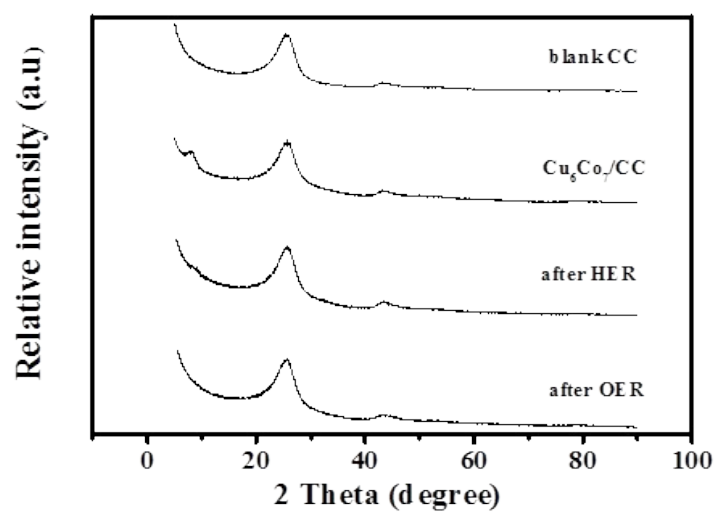


**Figure S8.** XRD spectra of Cu<sub>6</sub>Co<sub>7</sub>/CC after HER and OER tests.

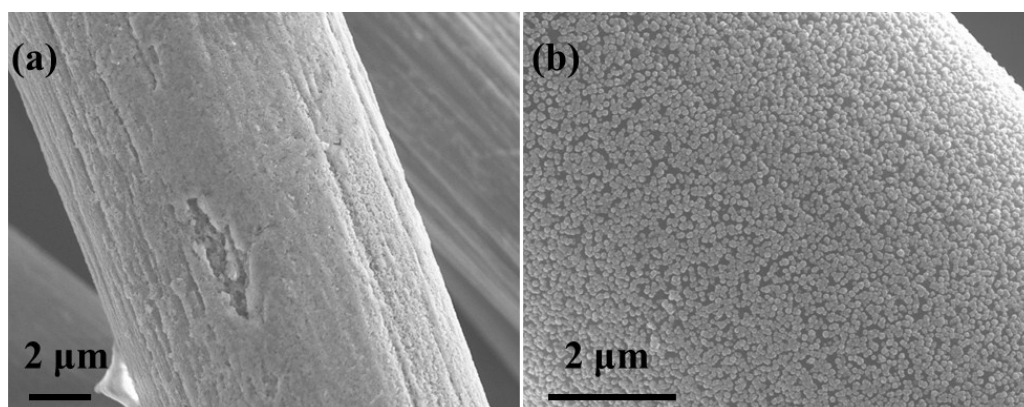


**Figure S9.** SEM images of Cu<sub>6</sub>Co<sub>7</sub>/CC after the overall water splitting reaction ( (a) anode, (b) cathode) .

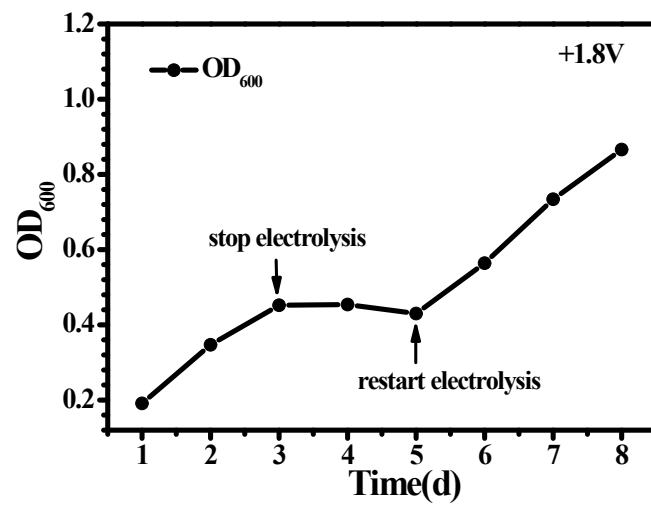


**Figure S10.** The dependence of the growth of *R. eutropha* on hydrogen evolution during the electrolysis with CO<sub>2</sub>. ( $E_{\text{appl}}=1.8 \text{ V}$ )

**Table S1.** Comparison of HER performances of different catalysts under neutral conditions.

Catalyst	Electrolyte	J <sup>a</sup> (mA cm <sup>-2</sup> )	η <sup>b</sup> (mV vs. RHE)	Tafel slope (mV dec <sup>-1</sup> )	Ref.
Cu <sub>6</sub> Co <sub>7</sub> /CC	pH 7	10	356	96	This work
		50	417		
		100	439		
H <sub>2</sub> -CoCat	pH 7	2.0	385	140	[1]
Co(bpbH <sub>2</sub> )Cl <sub>2</sub>	pH 7	1.0	1148	N/A	[2]
Co-HNP	pH 7	10	85	38	[3]
		100	237		
		50	180		
Co-S	pH 7	50	397	93	[4]
Carbon-armored					
Co <sub>9</sub> S <sub>8</sub> nanoparticle	pH 7	10	280	N/A	[5]
Cu(II) 1,2-ethylenediamine	pH 7	1.0	157	127	[6]
FeS, pyrrhotite	pH 7	0.7	450	150	[7]
Co <sub>9</sub> S <sub>8</sub> /CC	pH 7	10	175	N/A	[8]

		50	295		
Co-NRCNTs	pH 7	100	540	N/A	[9]

<sup>a</sup> Current density (mA cm<sup>-2</sup>)

<sup>b</sup> Overpotential (mV vs. RHE)

N/A These values were unavailable

#### References for **Table S1**:

[1] S. Cobo, J. Heidkamp, P.-A. Jacques, J. Fize, V. Fourmond, L. Guetaz, B. Jusselme, V. Ivanova, H. Dau, S. Palacin,; M. Fontecave, V. Artero, *Nat. Mater.* **2012**, *11*, 802.

[2] Z.-Q. Wang, L.-Z. Tang, Y.-X. Zhang, S.-Z. Zhan, J.-S. Ye, *J. Power Sources* **2015**, *287*, 50.

[3] B. Liu, L. Zhang, W. Xiong, M. Ma, *Angew. Chem. Int. Ed.* **2016**, *55*, 6725.

[4] Y. Sun, C. Liu, D. C. Grauer, J. Yano, J. R. Long, P. Yang, C. J. Chang, *J. Am. Chem. Soc.* **2013**, *135*, 17699.

[5] L.-L. Feng, G.-D. Li, Y. Liu, Y. Wu, H. Chen, Y. Wang, Y.-C. Zou, D. Wang, X. Zou, *ACS Appl. Mater. Interfaces* **2015**, *7*, 980.

[6] X. Liu, S. Cui, Z. Sun, P. Du, *Chem. Commun.* **2015**, *51*, 12954.

[7] C. Di Giovanni, W.-A. Wang, S. Nowak, J.-M. Grenèche, H. Lecoq, L. Mouton, M. Giraud, C. Tard, *ACS Catal.* **2014**, *4*, 681.

[8] L.-L. Feng, M. Fan, Y. Wu, Y. Liu, G.-D. Li, H. Chen, W. Chen, D. Wang, X. Zou, *J. Mater. Chem. A* **2016**, *4*, 6860.

[9] X. Zou, X. Huang, A. Goswami, R. Silva, B. R. Sathe, E. Mikmeková, T. Asefa, *Angew. Chem. Int. Ed.* **2014**, *53*, 4372.

**Table S2.** Comparison of the performance of Cu<sub>6</sub>Co<sub>7</sub>/CC to other bioelectrochemical systems for CO<sub>2</sub> fixation.

Cathode   Anode	Organism	E <sub>appl</sub>	Product	η <sub>elec</sub>	η <sub>SCE</sub>	Ref.
-----------------	----------	-------------------	---------	-------------------	------------------	------

Cu <sub>6</sub> Co <sub>7</sub> /CC	<i>R. eutropha</i> H16	1.8		41%	7.4%	This work
Cu <sub>6</sub> Co <sub>7</sub> /CC		2.0	Biomass	50%	9%	
		2.2		55%	9.9%	
Pt   Pt	<i>R. eutropha</i> H16	5.0	Biomass	4.8%	0.9%	[1]
CoP   CoPi	<i>R. eutropha</i> H16	2.0	Biomass	54%	9.7%	[2]
			PHB	36%	6.4%	
CoPi   SS	<i>R. eutropha</i> H16	3.0	Biomass	4.6%	0.8%	[3]
CoPi   NiMoZn	<i>R. eutropha</i> H16	2.7	Biomass	13%	2.3%	[3]
CoPi   SS	<i>R. eutropha</i> Re2133-pEG12	3.0	Biomass	4.6%	0.8%	[3]
Pt   In	<i>R. eutropha</i> LH74D	4.0	Biomass	1.8%	0.3%	[4]
Graphite   Graphite	<i>S. ovata</i>	3.0	acetate	30%	5.4%	[5]

References for **Table S2**:

[1] E. Schuster, H. G. Schlegel, *Arch. Mikrobiol.* **1967**, *58*, 380.



- [2] C. Liu, B. C. Colón, M. Ziesack, P. A. Silver, D. G. Nocera, *Science* **2016**, 352, 1210.
- [3] J. P. Torella, C. J. Gagliardi, J. S. Chen, D. K. Bediako, B. Colón, J. C. Way, P. A. Silver, D. G. Nocera, *Proc. Natl. Acad. Sci. USA* **2015**, 112, 2337.
- [4] H. Li, P. H. Opgenorth, D. G. Wernick, S. Rogers, T. Y. Wu, W. Higashide, P. Malati, Y. X. Huo, K. M. Cho, J. C. Liao, *Science* **2012**, 335 , 1596.
- [5] C. G. S. Giddings, K. P. Nevin, T. Woodward, D. R. Lovley, C. S. Butler, *Front. Microbiol.* **2015**, 6.